Article

J. Mex. Chem. Soc. **2008**, *52(4),* 249-255

ISSN 1870-249X

Electrochemical Treatment of Synthetic Wastewaters Containing Alphazurine A Dye: Role of Electrode Material in the Colour and COD Removal

José L. Nava,[1*] Marco A. Quiroz,[2] and Carlos A. Martínez-Huitle[3*]

[1] Departamento de Química, Universidad Autónoma Metropolitana-Iztapalapa. Av. San Rafael Atlixco 186, Vicentina, 09340, México, D.F., México.

[2] Departamento de Química y Biología, Universidad de las Américas-Puebla. Sta. Catarina Mártir, Cholula 72820, Puebla, México.

[3] University of Milan, DiSTAM, Laboratory of Electrochemistry, via Celoria 2, 20133, Milan, Italy.
jlnm@xanum.uam.mx, carlos.martinez@unimi.it

Received July 4, 2008; accepted November 25, 2008

Abstract. The electrochemical oxidation of Alphazurine A (αzA) has been studied in Na_2SO_4 media at Ti/IrO_2, Pb/PbO_2 and boron-doped diamond (Si/BDD) electrodes by bulk electrolysis experiments under galvanostatic control at j = 30 and 60 mA cm^{-2}. The obtained results have clearly shown that the electrode material plays an important role for the electrochemical incineration of αzA, where Pb/PbO_2 and Si/BDD lead complete mineralization of dye, while Ti/IrO_2 disfavoured such process. The complete mineralization of ±zA on Pb/PbO_2 and Si/BDD is due to the production of hydroxyl radicals on these materials surfaces. Current efficiencies obtained at Ti/IrO_2, Pb/PbO_2 and Si/BDD gave values of 3, 24 and 42%, for each electrode material, at 30 mA cm^{-2}, respectively. These values were higher than those obtained at 60 mA cm^{-2}. Energy consumption values from the electrolyses performed at 30 mA cm^{-2} were 254, 124 and 51 kWh m^{-3}, for Ti/IrO_2, Pb/PbO_2 and Si/BDD, respectively. UV spectrometric measurements showed faster αzA elimination at the Si/BDD electrode than those obtained on Ti/IrO_2 and Pb/PbO_2.
Keywords: Anodic oxidation, dyes, boron doped diamond electrode, iridium dioxide electrode, lead dioxide electrode.

Resumen. Se estudió la oxidación electroquímica del colorante Alfazurina A (αzA) en medio acuoso de Na_2SO_4 con electrodos de Ti/IrO_2, Pb/PbO_2 y diamante dopado con boro (Si/BDD), a través de experimentos de electrólisis, en modo galvanostático a j = 30 y 60 mA cm^{-2} . Los resultados obtenidos en este trabajo mostraron que el material del electrodo desempeña un papel importante para la incineración electroquímica del colorante αzA, indicando que los electrodos de Pb/PbO_2 y Si/BDD permiten la completa degradación del colorante, mientras que el electrodo de Ti/IrO_2 desfavorece tal proceso. La completa degradación del colorante αzA en los electrodos de Pb/PbO_2 y Si/BDD fue debida a la formación de radicales hidroxilo en la superficie de estos materiales. Los valores de las eficiencias de corriente fueron de 3, 24 y 42%, para Ti/IrO_2, Pb/PbO_2 y Si/BDD, respectivamente, a j = 30 mA cm^{-2}. . Estos valores fueron mayores que los obtenidos a 60 mA cm^{-2}. Por otro lado, el consumo de energía a j = 30 mA cm^{-2} presentó valores de 254, 124 and 51 kWh m^{-3} para los electrodos de Ti/IrO_2, Pb/PbO_2 y Si/BDD, respectivamente. La cinética de eliminación de color empleando el electrodo de Si/BDD fue mayor que la obtenida con los electrodos de Ti/IrO_2 y Pb/PbO_2.
Palabras clave: Oxidación anódica, colorantes, electrodos de diamante dopados con boro, electrodo de dióxido de iridio, electrodo de dióxido de plomo.

1. Introduction

Synthetic dyes are extensively used in many fields of up to-date technology, such as in various branches of the textile industry [1-4], leather tanning industry, paper production, food technology, agricultural research, light-harvesting arrays, photo-electrochemical cells, and in hair colourings. Different chemical classes of dyes are frequently employed on industrial scale such as the azo, anthraquinone, sulfur, indigo, triphenylmethyl (trityl), and phthalocyanine derivatives [1-4]. Due to large-scale production and extensive application, synthetic dyes can cause considerable environmental pollution and are serious health-risk factors [5], increasing of coloured wastewaters containing toxic and non biodegradable organic pollutants discharged in the environment. For this reason, powerful oxidation methods are needed to be applied to ensure the complete decolourization and degradation of dyestuffs and their metabolites present in the spent dyeing baths.

A wide range of methods has been developed for the removal of synthetic dyes from waters and wastewaters to decrease their impact on the environment. The technologies involve adsorption on inorganic or organic matrices, decolourization by photocatalysis, and/or by oxidation processes, microbiological or enzymatic decomposition, among others [1, 5, 6, 7]. Colour is usually the first contaminant to be recognized in wastewater and a very small amount of dye in water is highly visible and affects, water transparency and gas solubility of water bodies. The treatment of wastewater containing dyes and its decolourization involves serious problems, such as lower efficiency in colour removal and mineralization. Therefore, it is necessary to find an effective method of wastewater treatment capable of removing colour and degrading toxic organic compounds from industrial effluents.

Electrochemical processes for wastewater treatment are benefiting from advantages such as versatility, environmental compatibility and potential cost effectiveness among others described by other authors [8, 9]. Electrochemistry offers promising approaches for the prevention of pollution problems in the process industry. During the last two decades, research work has focused on the efficiency for oxidizing various pollutants at different electrodes, the improvement of the electrocatalytic activity and electrochemical stability of the electrode

materials, and the investigation of factors affecting the process performance and kinetics of pollutant degradation [9]. Metal oxides such as IrO_2 and RuO_2 known as «active» electrodes have been studied [9], achieving an incomplete oxidation of organic pollutants; whereas «non-active» oxides, such as Ti/SnO_2 and Pb/PbO_2 and their doped analogues are capable to oxidize organics to CO_2 [9, 10]. Within this last group of electrode materials, boron doped diamond electrodes have received great attention due to the wide range of their electrochemical properties [10].

In recent years, several scientific groups have investigated the application of diamond electrodes for removing dyes from wastewater [9, 10-16]. These anodes produce a huge amount of hydroxyl radicals (•OH) formed by water oxidation on Si/BDD surface, oxidizing the organic molecules in the proximity of the surface layer of •OH. The alternative path of a homogeneous reaction between the organic molecules and the ·OH confined within a reaction cage nearby the electrode surface. These hydroxyl radical exhibit strong oxidant properties by which complex colour molecules became degraded up to CO_2 [9, 10-16]; hence, they are promising anodes for industrial-scale wastewater treatment.

The aim of this work was to study the electrochemical oxidation for removing COD and colour of synthetic aqueous solutions containing triarylmethane dye such as alphazurine A (αzA), using three anodic materials (i.e. boron-doped diamond (Si/BDD), Pb/PbO_2 and Ti/IrO_2). This complex molecule (high molecular weight, many aromatic rings and different substituted groups) is presented in Figure 1. As it can be seen, the structural characteristics of αzA make very difficult the treatment of wastewaters containing this model dye by traditional processes. The influence of the current density and anode material, on the COD and colour removal, was investigated in order to identify optimal experimental conditions which gives high current efficiency and low energy requirements.

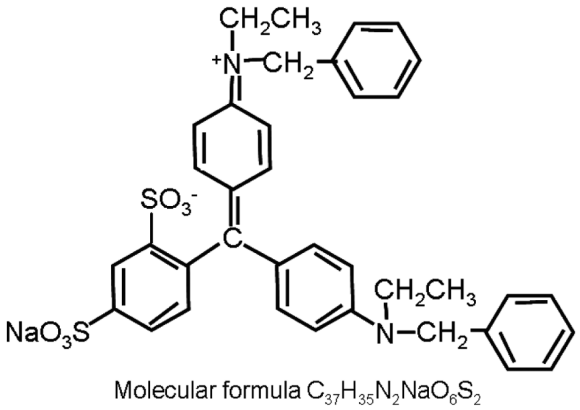

Fig. 1. General formula and molecular structure of αzA dye.

2. Experimental

a. Chemicals and Dye Solution

Ultrapure water was obtained by Simplicity water purification system. Chemicals were of the highest quality commercially available, and were used without further purification. Na_2SO_4 and H_2SO_4 were purchased from Fluka. The dyestuff solution was prepared dissolving different amounts of αzA in distilled wastewater containing 0.5 M Na_2SO_4.

b. Electrodes

Ti/IrO_2 electrodes were prepared by a sol-gel technique, which consisted of the following steps: dissolution in isopropanol of H_2IrCl_6 (10% solution), its brushing onto a pre-treated titanium base; drying at 80 °C; thermal decomposition at 530 °C. The above operation was repeated 10 times. The electrode films were eventually annealed for 2 hr at 530 °C. More details concerning anode preparation and characterization are given elsewhere [17].

The Pb/PbO_2 electrodes were prepared growing the anodic oxide at a current density of 10 mA cm^{-2}, in a 10% sulphuric acid solution and at 25 °C, during 90 min [18].

$$\begin{aligned} Pb + SO_4^{2-} &\rightarrow PbSO_4 + 2\,e \\ PbSO_4 + 2\,H_2O &\rightarrow PbO_2 + SO_4^{2-} + 4\,H^+ + 2\,e \end{aligned} \qquad (1)$$

$$Pb + 2\,H_2O \xrightarrow{4F} PbO_2 + 4\,H^+ + 4\,e$$

The boron doped diamond (Si/BDD) thin-film electrode was supplied by Adamant Technologies$^{T.M.}$ (Neuchatel, Switzerland). It was synthesized by hot filament chemical vapour deposition technique (HF CVD) on single crystal p-type Si <100> wafers (1–3 mΩcm, Siltronix). The filament temperature ranged from 2440 to 2560 °C, while the substrate temperature was 830 °C. The reactive gas was methane in excess dihydrogen (1% CH_4 in H_2). The dopant gas was trimethylboron with 3 mg dm^{-3} concentration. The gas mixture was supplied to the reaction chamber at a flow rate of 5 $dm^3\ min^{-1}$, with a diamond layer growth rate of 0.24 μm h^{-1}. The obtained diamond film had 1 μm thickness, with 10–30 mW cm resistivity. Typical Si/BDD surface topologies by atomic force microscopy (AFM) was obtained (Figure 2); a Nanoscope IIIa Scanning Probe microscope controller connected with a nanoscope multimode SPM, both from Digital Instruments were adopted for AFM analysis.

c. Electrochemical Measurements

Potentiodynamic measurements (polarization curves and cyclic voltammetry) were carried out at 25°C in a conventional three-electrode cell using model 1030 multi-potentiostat (CH Instruments, USA) connected to a PC. Ti/IrO_2, Pb/PbO_2 and Si/BDD have been used as working electrode, a saturated calomel electrode (SCE) as a reference and Pt wire as a counter

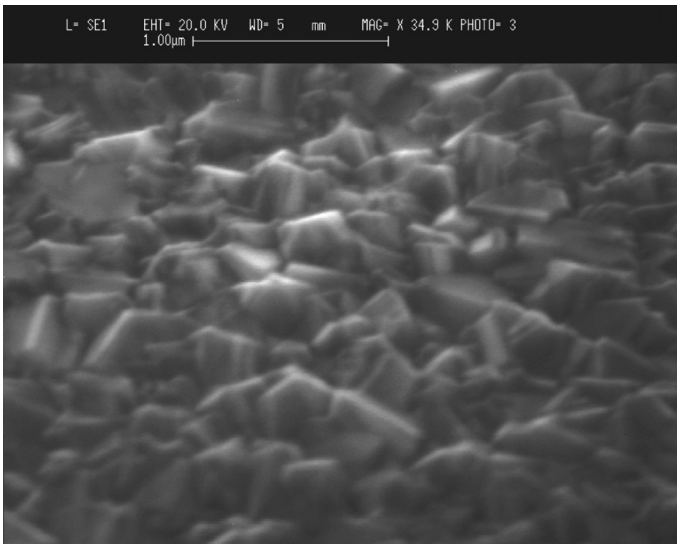

Fig. 2. Si/BDD images carried out by the AFM technique.

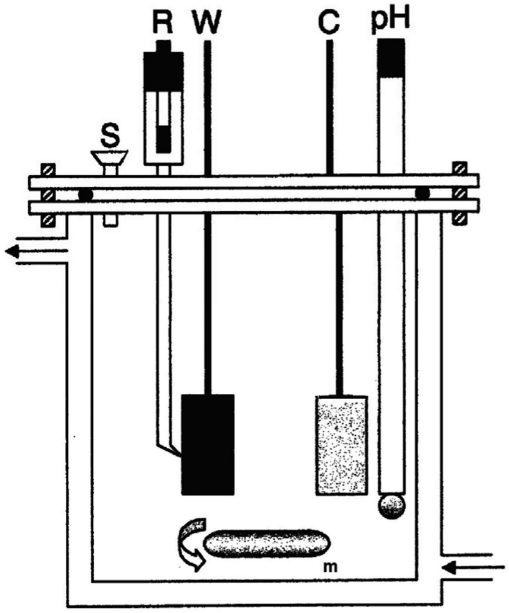

Fig. 3. Diagram of the one-compartment electrochemical cell used for studying anodic oxidation of αzA: C, counter, R, reference, and W, working electrodes, respectively; pH electrode; S, sample holder; and m, magnetic stirrer.

electrode. The exposed apparent area of the working electrodes was 1.5 cm^2.

Bulk oxidations were performed in a one-compartment electrochemical cell, the reaction compartment having a capacity of 500 mL. A schematic drawing of the experimental apparatus is shown in Fig. 3. The experiments of αzA oxidation were performed under galvanostatic conditions using a Tacussel model PJT24 potentiostat/galvanostat. Pb/PbO_2, Ti/IrO_2 and Si/BDD were used as the anodes, and zirconium as the cathode. Both electrodes were square, each with 10 cm^2 geometrical area (back area of each flat electrode was covered by inert polymeric film to avoid the interaction with the electrolyte solution). Reagent grade chemicals and three fold distilled water (16-18 MW) were used throughout the work. The set of electrolysis were performed at the same temperature values of microelectrolysis experiments.

d. Analytical Methods

Colour removal was monitored by measuring absorbance decrease (λ = 637 nm), using a Hach Model DR/4000 V UV-Vis spectrophotometer. Solution COD data were obtained with the same spectrophotometer after digestion of samples in a Merck Model TR-300 thermoreactor. Current efficiency (CE) for anodic oxidation of αzA was calculated from COD values, using the following relationship [9]:

$$\%CE = FV\left(\frac{\left[COD_0 - COD_t\right]}{8I\ t}\right)\times 100 \qquad (2)$$

where COD_0 and COD_t are chemical oxygen demands at times $t = 0$ (initial) and t (in g O_2 dm^{-3}), respectively, I the current (A), F the Faraday constant (96,487 C mol^{-1}), V the electrolyte volume (dm^3), and 8 is the oxygen equivalent mass (g $eq.^{-1}$).

The energy consumption for the removal of one Kg of COD is calculated and expressed in KWh m^{-3}. The average cell voltage, during the electrolysis, is taken for calculating the energy consumption, as follows [9]:

$$\text{Energy consumption} = \left(\frac{\left[\left[tVA/Sv\right]/1\ \ 10^3\right]}{COD/1\ \ 10^6}\right) \qquad (3)$$

where t is the time of electrolysis (h); V and A are the average cell voltage and the electrolysis current (V and A, respectively); Sv is the sample volume (dm^3), and ΔCOD is the difference in COD (in gO_2 dm^{-3}).

3. Results and Discussion

a. Electrochemical Measurements

Preliminary experiments have been carried out by polarization curves and cyclic voltammetry, to obtain information on the electroactivity of αzA at electrodes, like Ti/IrO_2, Pb/PbO_2 and Si/BDD, prior to anodic oxygen evolution. Fig. 4 shows linear polarization curves of a Ti/IrO_2, Pb/PbO_2 and Si/BDD electrodes obtained in 1 M Na_2SO_4 with a scan rate of 50 mV s^{-1}, which started form the open circuit potential (OCP). The curves (a, b and c) are very different and show that oxygen evolution potential increases from 1.3 V to 1.8 V and to 2.4 V versus SCE for Ti/IrO_2, Pb/PbO_2 and Si/BDD [18], respectively. This means that Ti/IrO_2 has low oxygen evolution overpotential and consequently is good electrocatalysts for the

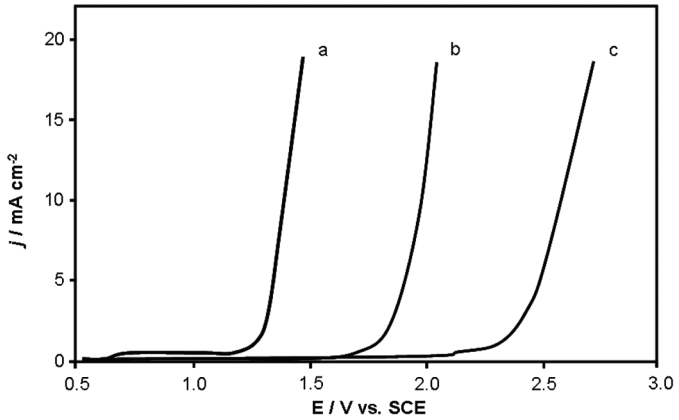

Fig. 4. Polarization curves: a) Ti/IrO_2, b) Pb/PbO_2 and c) Si/BDD electrodes obtained in 1 M Na_2SO_4 with a scan rate of 50 mV s^{-1}. Electrode area: 1.5 cm^2

oxygen evolution reaction, while Pb/PbO_2 and Si/BDD have high oxygen evolution overpotential and consequently are poor electrocatalysts for the oxygen evolution reaction [18].

Voltammograms were obtained at 50 mg dm^{-3} of concentration of dye, in acidic media (Na_2SO_4 0.5 M) and at room temperature (25 °C). In all cases, the CV curves were recorded below the decomposition potential of water and/or supporting electrolyte. Fig. 5 shows the cyclic voltammograms (CV) for background electrolyte and for solution containing 50 mg dm^{-3} of αzA dye at different anode materials. CV curves obtained with a Ti/IrO_2 in Na_2SO_4 0.5 M (Fig. 5A), presented the typical behaviour of thermally prepared oxide layer. The shape in the CV with not well-defined peaks can be understood in terms of a large heterogeneity in the surface site and superposition of the redox processes for the transition lower metal oxide/higher metal oxide. During the first cycle, in the solution containing αzA (Fig. 5A) a broad anodic peak at approximately +0.7 V *vs*. SCE, corresponding to direct oxidation of αzA appeared and the current intensity at a given potential in the region of supporting electrolyte decomposition decreased. This last suggests the inhibition for the oxygen evolution reaction due to the partial deactivation of the active sites on the Ti/IrO_2 surface. Therefore, the addition of the organic substrate does not seem to have a significant effect on the shape of CV curve, with the exception of a very small increase of currents in the oxygen evolution potential range.

A very different behaviour was observed at the Pb/PbO_2 electrode, where, as shown in Fig. 5B, a significant current shift could be recorded when αzA was added to the solution, compared with the curves recorded in 0.5 M Na_2SO_4, at the same *j* value. This indicates that the pathway of αzA oxidation involves water decomposition intermediates, mainly hydroxyl radicals, which are only available in conditions of oxygen evolution rather than direct electron transfer from the substrate.

As shown in the Fig. 5C, at voltammograms obtained on Si/BDD anode, during the first scan in presence of αzA, two anodic current peaks corresponding to the direct oxidation of

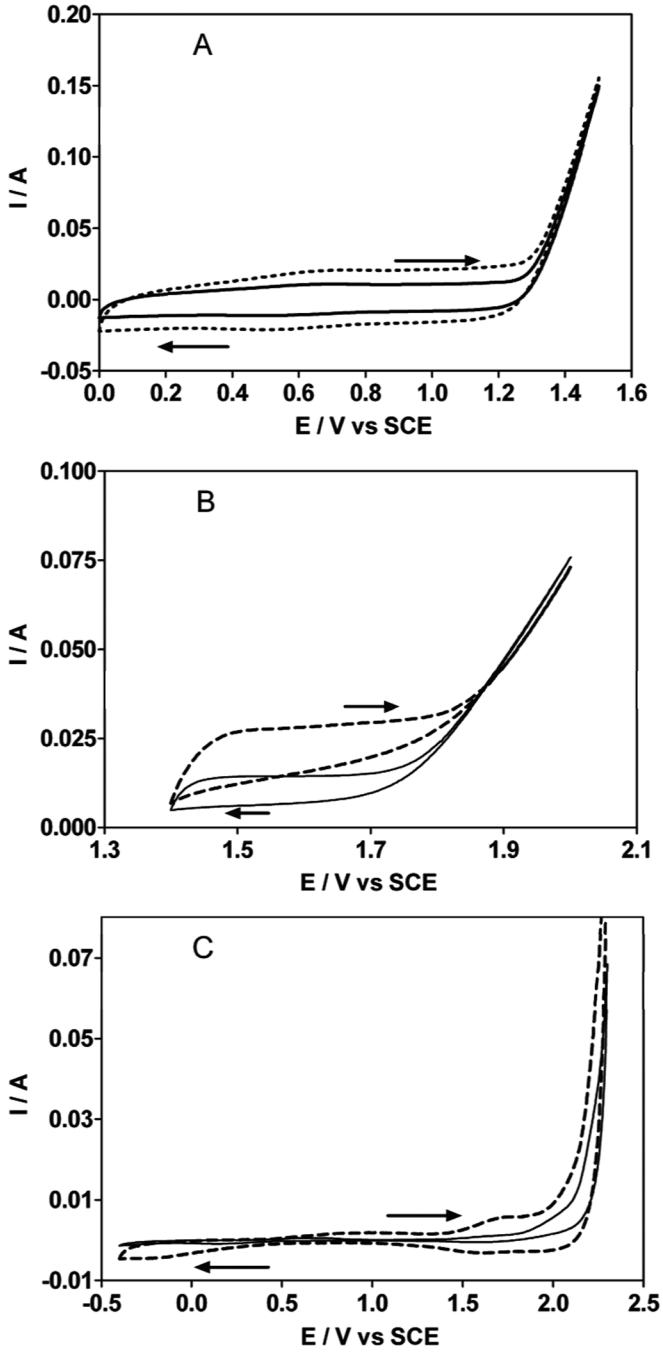

Fig. 5. Voltammograms in presence of 50 mg dm^{-3} of αzA solution in 0.5 M Na_2SO_4 at different electrode materials. The bold line represents the supporting electrolyte and dash line represents the first cyclic voltammogram. Scan rate 100 mV s^{-1}, T = 25°C. Anodes: (A) Ti/IrO_2; (B) Pb/PbO_2; and (C) Si/BDD

αzA are observed at about +1.0 and +1.5 V vs. SCE. As in the case of Ti/IrO_2, this decrease in electrode activity appears to be due to deposition of aromatic polymeric products on the electrode surfaces. Similar behaviour for the anodic oxidation of other aromatic compounds on Si/BDD electrode already

described and discussed in the literature [9, 10-15]. It is important to remark that, Si/BDD surface rapidly regained the initial activity and the polymeric film is destroyed by simple polarization at high anodic potential (E > 2.3V versus SCE) in the region of water decomposition, allowing the production of hydroxyl radicals that oxidize the polymeric film on their surface.

b. Galvanostatic Oxidation Experiments

At all the electrode materials taken into consideration in this work, αzA anodic oxidation experiments were performed under galvanostatic conditions, allowing a more complete description of the role of electrode surfaces and current densities in electrochemical wastewater treatments. During each electrolysis experiment, the αzA dye degradation was followed by spectrophotometric and COD methods.

The anodic oxidations of 500 ppm COD of αzA in 0.5 M Na_2SO_4 have been performed with Ti/IrO_2, Pb/PbO_2 and Si/BDD applying current densities of 30 and 60 mA cm^{-2}. The results presented in Figures 6 and 7 show that the COD removal and the average current efficiency (CE) are strongly influenced by the anode material.

At Ti/IrO_2 oxide only a small COD reduction (Figure 6) and a low current efficiency (Figure 7) were attained. In fact, as shown by the potentiodynamic measurements (Figure 5A), this anode material displayed low activity for αzA dye oxidation, favouring a secondary reaction: oxygen evolution reaction instead of αzA dye oxidation. This behaviour can be explained according to the mechanism proposed by Comninellis [19], who suggested that when, like in the case of IrO_2, metal cations in the oxide lattice may reach higher oxidation states under anodic polarization (active electrodes) a stabilization of adsorbed •OH radicals takes place, which favours the oxygen evolution at the expense of the electrochemical incineration reaction. As shown by these CE *vs.* time curves, Figure 7, the lowest CE values were obtained on Ti/IrO_2. These values confirm that this electrode material favours the oxygen evolution reaction instead anodic oxidation of the organic molecule.

As shown in Figure 6, interesting results were obtained at the Pb/PbO_2 electrodes; in this case, a nearly complete elimination of αzA was observed by applying a current density of 60 mA cm^{-2}; although the faradaic efficiency of the initial stages of oxidation process is quite low, Figure 7. For j = 30 mA cm^{-2}, the oxidative attack is faster in its first-intermediate part, allowing a practically complete mineralization of organics with essentially the same charge consumption. As shown by CE *vs.* time curves in Figure 7, a highest CE value (~25) was obtained at 30 mA cm^{-2} while at 60 mA cm^{-2} the CE were about 8.5. The low CE value obtained at high current density can be due to mass transport limitations. It is important to point out that in this paper did not show the influence of flow on the rate of mineralization. Nevertheless, Polcaro et al. [20] reported studies carried out in an undivided impinging-jet flow cell at different Reynolds values during the electrochemical incineration of phenol on BDD anodes, indicating that convection increases the rate of mineralization and, consequently, it improves the CE. This outcome is in agreement with the data recently published by Nava et al. [21]. They showed that hydrodynamics in a FM01-LC cell improves hydroxyl-organic contact at the BDD surface, a phenomenon that increases organic current mineralization efficiency. It is important to mention that authors have considered to use a flow cell for future investigations in order to improve the performance of the electrochemical incineration processes.

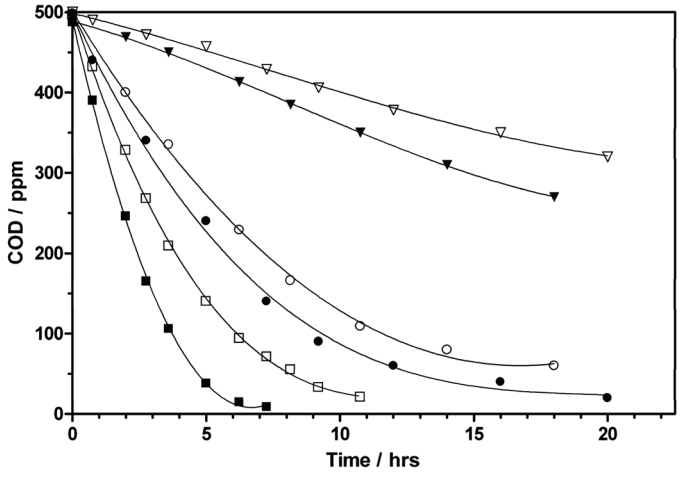

Fig. 6. αzA dye degradation on different anode materials as a function of the electrolysis time and the applied current density. Ti/IrO_2 (▽) 30 mA cm^{-2} and (▼) 60 mA cm^{-2}, Pb/PbO_2 (○) 30 mA cm^{-2} and (●) 60 mA cm^{-2} and Si/BDD (□) 30 mA cm^{-2} and (■) 60 mA cm^{-2}. Experimental conditions: 25°C and 500 ppm of αzA dye concentration.

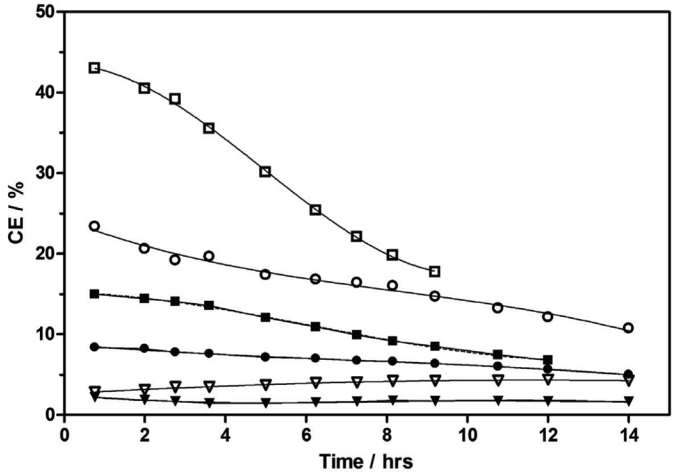

Fig. 7. Comparison of the trend of current efficiency (CE) as function of time, during the oxidation of αzA (0.5 M Na_2SO_4) at different anodes. Ti/IrO_2 (▽) 30 mA cm^{-2} and (▼) 60 mA cm^{-2}, Pb/PbO_2 (○) 30 mA cm^{-2} and (●) 60 mA cm^{-2} and Si/BDD (□) 30 mA cm^{-2} and (■) 60 mA cm^{-2}.

On the other hand, Figures 6 and 7 show that Si/BDD allowed an oxidation rate and CE higher than PbO_2 and Ti/IrO_2 electrodes. This behaviour can be explained by the different reactivity of the electrogenerated hydroxyl radicals. Si/BDD anode, which is well known to have weak adsorption properties due to its inert surface, hydroxyl radicals are very weakly adsorbed and consequently they are very reactive toward organics oxidation (non-active electrode) [20-31].

It has been suggested [9, 12, 23] that, at Si/BDD electrodes, the $^{\bullet}OH$ radicals formed by water oxidation (equation 4) can be either electrochemically oxidized to oxygen (equation 5) or contribute to the complete oxidation of the organic compounds, in this case dyes (equation 6):

$$H_2O \rightarrow (^{\bullet}OH)_{ads} + H^+ + e \quad (4)$$

$$(^{\bullet}OH)_{ads} \rightarrow \frac{1}{2}O_2 + H^+ + e \quad (5)$$

$$\text{Organic molecules} \xrightarrow{(^{\bullet}OH)_{ads}} CO_2 + H_2O \quad (6)$$

Other oxidants formed at the diamond surface ($H_2S_2O_8$, O_3) can participate in the oxidation of the carboxylic acids, in the proximity of the electrode surface and/or in the bulk of the electrolyte. Peroxodisulphates have been demonstrated to be formed in solutions containing sulphates [25,26], during electrolysis with Si/BDD electrodes (equation 7):

$$2SO_4^{2-} \rightarrow S_2O_8^{2-} + 2e^- \quad (7)$$

These reagents are known to be very powerful oxidants and can oxidize organic matter leading to an increase in COD and colour removal rates. These results are in agreement with those obtained by other authors [25, 26].

On the contrary, PbO_2 is hydrated and hydroxyl radicals are expected to be more strongly adsorbed on its surface and consequently less reactive. Similar results were also reported in [18] for the oxidation of chloranilic acid. From the data reported in Figure 6, at PbO_2 and Si/BDD anodes, the COD decreased close to zero, meaning the complete oxidation of αzA dye and all its metabolites. These results are in agreement with those of the preliminary electrochemical measurements described in Figure 5, indicating that with the use of PbO_2 and Si/BDD electrodes αzA is incinerated by direct electron transfer and by reaction with $^{\bullet}OH$ radicals electrogenerated from water discharge. Finally, in the case of Si/BDD, highest CE values were obtained with regard to other anodic materials.

The oxidation of the αzA on the Ti/IrO_2, Pb/PbO_2 and Si/BDD electrodes was also monitored by spectrophotometric measurements. The absorption spectra of αzA at room temperature present an absorption band at about 637 nm which is directly related to the colour of the solution. Fig. 8 shows the changes of absorbance during the electrolysis carried out at a current of 30 mA cm^{-2}. As can be seen in Fig. 8, only a small decrease of the absorbance was obtained at Ti/IrO_2, while at PbO_2 and Si/BDD electrodes the removal of colour was complete, which is in agreement with the evolution of the COD (Figure 6), where the anodic oxidation and colour removal were faster at Si/BDD than Pb/PbO_2 anode.

c. Energy Consumption

Finally, an estimation of the energy consumption (kWh m^{-3}) for COD removal during electrochemical oxidation of a solution of αzA dye was calculated (ca. 90% of COD elimination for Si/BDD and PbO_2 anodes, while 60% of COD decay for IrO_2 electrode). According to Fig. 9, Si/BDD electrode presents low values of the energy consumption respect to the other anodic materials. Even if the PbO_2 anode showed good performances for removing colour and COD from solution, this electrode achieved higher values of the energy consumption. Further, although complete COD removal is technically feasible, its high-energy cost makes this technique unsuitable for a refining process, but it is important to remark that this technique could be used to eliminate the colour as a pre-treatment.

It is important to mention that the studies proposed in this paper have been performed in batch cell with parallel plate electrodes, where convection, supplied by magnetic stirrer, disfavours mass transport giving modest current efficiencies and high energy consumption values; however this analysis should serve as a useful starting point at which a flow cell, such as the FM01-LC electrolyser, may be latter incorporated, whose hydrodynamics, mass transport, and cell configuration, guarantee high current efficiency and low E_{cell}, giving low energy consumption [21, 30].

4. Concluding Remarks

Electrochemical treatment of a synthetic solution containing αzA dye was investigated using Si/BDD, Pb/PbO_2 and Ti/IrO_2 anodes. The influence of current density on COD and colour

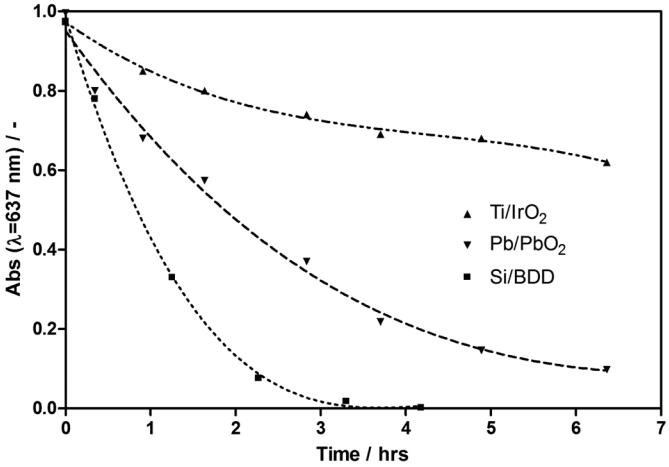

Fig. 8. Colour removal on different anode materials as a function of the electrolysis time. Experimental conditions: 25°C, 500 ppm of αzA dye concentration and applied current density of 30 mA cm^{-2}.

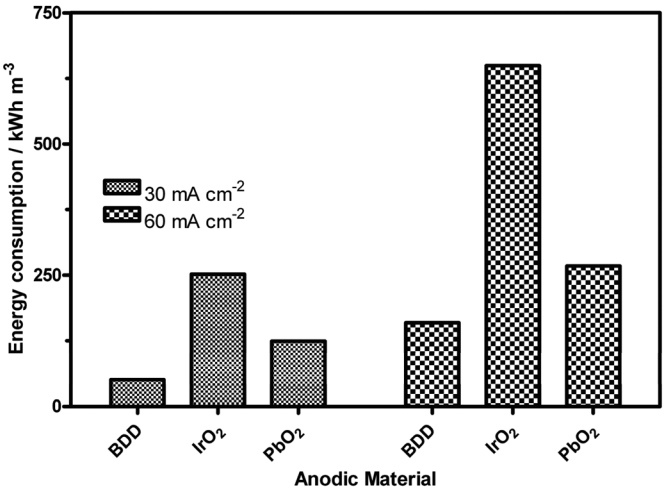

Fig. 9. Estimation of the energy consumption for all anodic materials at different current densities applied. Values of the energy consumption at BDD and PbO_2 anodes were estimated after 90% of the dye oxidation. In the case of IrO_2 anode, values were estimated after 60% of the dye oxidation, according to data presented in Figure 6.

removal was analysed and the following conclusions can be drawn:

These results showed in general that the dye elimination depends on the nature of the electrode material, and it is dependent on the applied current density and electrolysis time. Thus, the removal efficiency of αzA dye follows the next order: Si/BDD >> Pb/PbO_2 > Ti/IrO_2; being at Si/BDD electrode at which the best COD and colour removal efficiencies were attained (up to 95% of COD decay after 9 h, and 100% decolourization after 5 h), due to the formation of hydroxyl radicals from the water discharge and also, the probable participation of strong oxidant species such as peroxidisulphates. Pb/PbO_2 and Si/BDD lead complete mineralization of dye, while Ti/IrO_2 disfavoured such process. The complete mineralization of αzA on Pb/PbO_2 and Si/BDD is due to the production of hydroxyl radicals on these materials surfaces. Current efficiencies obtained at Ti/IrO_2, Pb/PbO_2 and Si/BDD gave values of 3, 24 and 42%, for each electrode material, at 30 mA cm^{-2}, respectively. These values were higher than those obtained at 60 mA cm^{-2}. Energy consumption values from the electrolyses performed at 30 mA cm^{-2} were 254, 124 and 51 kWh m^{-3}, for Ti/IrO_2, Pb/PbO_2 and Si/BDD, respectively. The significance of these results are even greater having in mind that results obtained with other advanced oxidation methods require long times treatment and generates more products of oxidation [31]. A probable industrial application of the electrochemical oxidation processes for the total elimination and/or reduction of the control levels of dyes discharges are clearly justifiable

References

1. Forgacsa, E.; Cserhati, T.; Oros, G. *Environ. International* **2004**, *30*, 953– 971.
2. Gupta, G. S.; Shukla, S. P.; Prasad, G.; Singh, V. N. *Environ. Technol.* **1992**, *13*, 925– 936.
3. Shukla, S. P.; Gupta, G. S. *Ecotoxicol. Environ. Saf.* **1992**, *24*, 155– 163.
4. Sokolowska-Gajda, J.; Freeman, H. S.; Reife, A. *Dyes and Pigments* **1996**, *30*, 1–20.
5. Robinson, T.; McMullan, G.; Marchant, R.; Nigam, P. *Bioresource Technol.* **2001**, *77*, 247-255.
6. Shaul, G. M.; Holdsworth, T. J.; Dempsey, C. R. Dostal K. A. *Chemosphere* **1991**, *22*, 107–19.
7. Hao, O. J.; Kim, H.; Chiang, P. C. *Crit. Rev. Environ. Sci. Technol*. **2000**, *30*, 449–502.
8. Rajeshwar, K.; Ibanez, J. G.; Swain, G. M. *J. Appl. Electrochem.* **1994**, *24*, 1077–1091.
9. Martínez-Huitle, C. A.; Ferro, S. *Chem. Soc. Rev.* **2006**, *35*, 1324-1340.
10. Martinez-Huitle, C. A.; Quiroz, M. A. *J. Environ. Eng. Manage.* **2008**, *18*, 155-172.
11. Fernandes, A.; Morao, A.; Magrinho, M.; Lopes, A.; Goncales I. *Dyes and Pigments* **2004**, *61*, 287-296.
12. Cañizares, P.; Gadri, A.; Lobato, J.; Bensalah, N.; Rodrigo, M.-A.; Sáez C. *Ind. Eng. Chem. Res.* **2006**, *45*, 3468-3473.
13. Faouzi, M.; Cañizares, P.; Gadri, A.; Lobato, J.; Bensalah, N.; Paz, R.; Rodrigo, M. A.; Sáez, C. *Electrochim. Acta* **2006**, *52*, 325-331.
14. Ahmadi, M. F.; Bensalah, N.; Gadri, A. *Dyes and Pigments* **2007**, *73*, 86-89.
15. Panizza, M.; Cerisola, G. *J. Hazard. Mat.* **2008**, *135*, 83-88.
16. Butrón, E.; Juárez, M. E.; Solis, M.; Teutli, M.; González, I.; Nava, J. L. *Electrochim. Acta* **2007**, *52*, 6888-6894.
17. Vercesi, G. P.; Salamin, J. Y.; Comninellis, Ch. *Electrochim. Acta*, 36 (1991) 991-998.
18. Martínez-Huitle, C. A.; Quiroz, M. A.; Comninellis, Ch.; Ferro, S.; De Battisti, A. *Electrochim. Acta* **2004**, *50*, 949–956.
19. Comninellis, Ch. *Electrochim. Acta* **1994**, *39*, 1857-1862.
20. Polcaro, A. M.; Vacca, A.; Palmas, S.; Mascia, M. *J. Appl. Electrochem.* **2003**, *33*, 885–892.
21. Nava, J. L.; Butrón, E.; González, I. *J. Environ. Eng. Manag*. **2008**, *18*, 221-230.
22. Canizares, P.; Garcia-Gomez, J.; Saez, C.; Rodrigo, M.A. *J. Appl. Electrochem*. **2004**, *34*, 87–94.
23. Marselli, B.; García-Gómez, J.; Michaud, P.A.; Rodrigo, M.A.; Comninellis, Ch. *J. Electrochem. Soc.* **2003**, *150*, D79-D83.
24. Michaud, P.A.; Panizza, M.; Ouattara, L.; Diaco, T.; Foti, G.; Comninellis, Ch. *J. App. Electrochem.* **2003**, *33*, 151-154.
25. Michaud, P.-A.; Mahé, E.; Haenni, W.; Perret, A.; Comninellis, Ch. *Electrochem. Solid State Lett.* **2000**, *3*, 77-83.
26. Cañizares, P.; Larrondo, F.; Lobato, J.; Rodrigo, M.-A.; Sáez, C. *J. Electrochem. Soc*. **2005**, *152*, D191-D196.
27. Panizza, M.; Michaud, P.A.; Cerisola, G.; Comninellis, C. *J. Electroanal. Chem.* **2001**, *507*, 206.
28. Rodrigo, M.A.; Michaud, P.A.; Duo, I.; Panizza, M.; Cerisola, G.; Comninellis, C. *J. Electrochem. Soc.* **2001**, *148*, D60–D64.
29. Canizares, P.; Saez, C.; Lobato, J.; Rodrigo, M. A. *Ind. Eng. Chem. Res.* **2004**, *43*, 1944–1951.
30. Nava, J. L.; Núñez, F.; González, I. *Electrochim. Acta* **2007**, *52*, 3229-3235.
31. Martinez-Huitle, C. A.; Brillas, E. *Appl. Catal. B, Environ*. **2008**, in press, doi:10.1016/ j.apcatb.2008.09.017..